Development 128, 4801-4813 (2001)
Printed in Great Britain © The Company of Biologists Limited 2001
DEV2798

OTD/OTX2 functional equivalence depends on 5′ and 3′ UTR-mediated control of *Otx2* mRNA for nucleo-cytoplasmic export and epiblast-restricted translation

Dario Acampora[1,2,‡], Pietro Pilo Boyl[1,‡], Massimo Signore[1], Juan Pedro Martinez-Barbera[1], Cristina Ilengo[3], Eduardo Puelles[1], Alessandro Annino[2], Heinrich Reichert[4], Giorgio Corte[3,5] and Antonio Simeone[1,2,*]

[1]MRC Centre for Developmental Neurobiology, King's College London, Guy's Campus, New Hunts House, London SE1 9RT, UK
[2]International Institute of Genetics and Biophysics, CNR, Via G. Marconi 12, 80125 Naples, Italy
[3]IST-National Institute for Cancer Research, [5]Dipartimento di Oncologia Clinica e Sperimentale, Università di Genova, Largo Benzi, 16132 Genova, Italy
[4]Institute of Zoology, University of Basel, Rheinsprung 9, CH-4051 Basel, Switzerland
*Author for correspondence (e-mail: antonio.simeone@kcl.ac.uk)
‡These authors contributed equally to the work

Accepted12 September 2001

SUMMARY

How gene activity is translated into phenotype and how it can modify morphogenetic pathways is of central importance when studying the evolution of regulatory control mechanisms. Previous studies in mouse have suggested that, despite the homeodomain-restricted homology, *Drosophila orthodenticle* (*otd*) and murine *Otx1* genes share functional equivalence and that translation of *Otx2* mRNA in epiblast and neuroectoderm might require a cell type-specific post-transcriptional control depending on its 5′ and 3′ untranslated sequences (UTRs).

In order to study whether OTD is functionally equivalent to OTX2 and whether synthesis of OTD in epiblast is molecularly dependent on the post-transcriptional control of *Otx2* mRNA, we generated a first mouse model (*otd*^{2}) in which an *Otx2* region including 213 bp of the 5′ UTR, exons, introns and the 3′ UTR was replaced by an *otd* cDNA and a second mutant (*otd*^{2FL}) replacing only exons and introns of *Otx2* with the *otd* coding sequence fused to intact 5′ and 3′ UTRs of *Otx2*.

***otd*^{2} and *otd*^{2FL} mRNAs were properly transcribed under the *Otx2* transcriptional control, but mRNA translation in epiblast and neuroectoderm occurred only in *otd*^{2FL} mutants. Phenotypic analysis revealed that visceral endoderm (VE)-restricted translation of *otd*^{2} mRNA was sufficient to rescue *Otx2* requirement for early anterior patterning and proper gastrulation but it failed to maintain forebrain and midbrain identity.**

Importantly, epiblast and neuroectoderm translation of *otd*^{2FL} mRNA rescued maintenance of anterior patterning as it did in a third mouse model replacing, as in *otd*^{2FL}, exons and introns of *Otx2* with an *Otx2* cDNA (*Otx2*^{2c}). The molecular analysis has revealed that *Otx2* 5′ and 3′ UTR sequences, deleted in the *otd*^{2} mRNA, are required for nucleo-cytoplasmic export and epiblast-restricted translation. Indeed, these molecular impairments were completely rescued in *otd*^{2FL} and *Otx2*^{2c} mutants. These data provide novel in vivo evidence supporting the concept that during evolution pre-existing gene functions have been recruited into new developmental pathways by modifying their regulatory control.

Key words: *otd*, *Otx2*, UTR, Translational control, VE, Anterior patterning, Brain evolution, Mouse

INTRODUCTION

Early brain development in higher vertebrates is a complex process characterised by the induction and maintenance of the anterior neuroectoderm, which subsequently becomes regionalised into forebrain, midbrain and hindbrain (Beddington and Robertson, 1999). Further differentiation of these territories leads to the generation of neuronal populations with a restricted identity and specific functional properties (Lumsden, 1990; Lumsden and Krumlauf, 1996; Rubenstein et al., 1998).

In the last decade, a considerable amount of data has been collected on the role of developmental control of genes involved in brain morphogenesis in mammals. Most of them are the vertebrate homologues of *Drosophila* genes that encode transcription factors or signalling molecules (Lemaire and Kodjabachian, 1996; Holland, 1999; Rubenstein et al., 1998). Among these is the *orthodenticle* gene family, which includes the *Drosophila orthodenticle (otd)* and the murine *Otx1* and *Otx2* genes (Simeone et al., 1992; Simeone et al., 1993; Finkelstein and Boncinelli, 1994).

Previous studies have indicated that the *Otx* genes play an

important role in brain development [see reviews by Simeone and Acampora (Simeone, 1998; Acampora and Simeone, 1999; Simeone 2000; Acampora et al., 2001)]. These studies have established that *Otx2* is required in the VE for early induction of anterior neural patterning and proper gastrulation, and subsequently, in the epiblast-derived tissues such as axial mesendoderm (ame) and anterior neuroectoderm for maintenance of forebrain and midbrain regional identities (Acampora et al., 1995; Acampora et al., 1998b; Rhinn et al., 1998; Acampora and Simeone, 1999; Beddington and Robertson, 1999). In particular, the analysis of embryos replacing *Otx2* with the human *Otx1* (*hOtx1*) cDNA has also revealed that while the *hOtx1* mRNA is transcribed in both the VE and epiblast, the hOTX1 protein is synthesised only in the VE (Acampora et al., 1998b). This unexpected phenomenon has suggested the possibility that a differential post-transcriptional control may exist between VE and epiblast and that the *Otx2* replaced region, including 213 bp of the 5′ untranslated region (UTR), exons, introns and the 3′ UTR, may contain regulatory elements required for epiblast-restricted translation of *Otx2* mRNA. In terms of brain development this potential control of *Otx2* mRNA translation might represent a crucial aspect since lack or reduction of OTX2 protein is invariably associated with lack or reduction of the forebrain and midbrain.

In this context, we have very recently reported that embryos carrying a 300 bp insertion of exogenous DNA from the λ phage ($Otx2^{\lambda}$) into the *Otx2* 3′ UTR, exhibit severe brain abnormalities and drastic reduction of OTX2 protein for an impairment of $Otx2^{\lambda}$ mRNA to form efficient polyribosome complexes (Pilo Boyl et al., 2001).

However, although OTX1 and OTX2 appear to be equivalent in the VE and OTD/OTX1 properties largely overlap, it could not be predicted whether OTD is also equivalent to OTX2 in instructing proper brain morphogenesis.

Understanding how the genetic mechanisms that control brain morphogenesis have evolved represents a central aspect of comparative developmental biology. Despite the enormous morphological diversity between invertebrates and vertebrates, striking examples of functional conservation of genetic programmes for morphogenesis are found in these animal groups. Among these are the invertebrate *HOM-C* and vertebrate *Hox* genes which control the specification of axial patterning (Lewis, 1978; Krumlauf, 1994; Lumsden and Krumlauf, 1996), the *short gastrulation/Chordin* and *decapentaplegic*/*Bmp4* genes, which control dorsoventral (DV) patterning (De Robertis and Sasai, 1996) and the *Drosophila eyeless (ey)* and vertebrate *Pax6* genes, which control eye morphogenesis (Callaerts et al., 1997).

Recently, functional conservation among members of the *otd/Otx* group has been demonstrated in cross-phylum genetic rescue experiments (Acampora et al., 1998a; Leuzinger et al., 1998; Nagao et al., 1998; Sharman and Brand, 1998). Nevertheless, homeodomain-restricted homology between OTD and OTX2 proteins as well as the huge diversity existing between mouse and *Drosophila* early head morphogenesis suggest that *otd* should be unable to share functional equivalence with *Otx2* in VE (specification of the early anterior patterning and proper gastrulation) and neuroectoderm (maintenance of forebrain and midbrain identities).

In order to assess whether OTD is equivalent to OTX2 and, importantly, whether translation of *otd* mRNA requires *Otx2* post-transcriptional control in epiblast and neuroectoderm, we generated a first mouse model (otd^{2}) where an *otd* cDNA replaces an *Otx2* genomic region including 213 bp of the 5′ UTR, coding sequences, introns and the entire 3′ UTR. In a second mutant (otd^{2FL}), only the *Otx2* coding sequence and introns were replaced by the *otd* coding sequence. While the otd^{2} and otd^{2FL} expression was correctly driven by *Otx2* transcriptional control, mRNA translation in epiblast and neuroectoderm occurred only in otd^{2FL} mutants, being otd^{2} mRNA translation restricted only to VE. A third mutant ($Otx2^{2c}$) carrying an *Otx2* cDNA in place of the *Otx2* coding sequence and introns, was generated to compare OTD and OTX2 functions. Phenotypic analysis of otd^{2}, otd^{2FL} and $Otx2^{2c}$ homozygous mutants indicated that OTD fulfilled OTX2 functions required in VE and neuroectoderm for murine brain development when the two genes undergo the same genetic modifications. A detailed molecular analysis has indicated that the *Otx2* 5′and 3′ UTRs deleted in otd^{2} mutant were responsible for a severe impairment of both nucleo-cytoplasmic export and epiblast-restricted translation of the otd^{2} mRNA.

Importantly, these molecular abnormalities were completely rescued in otd^{2FL} and $Otx2^{2c}$ mutants and confirmed in $hOtx1^{2}$ embryos. In this study, we have shown that the *otd* mRNA is translated in epiblast and neuroectoderm only if the *Otx2* post-transcriptional control is provided, and then in turn, the OTD protein can perform OTX2 functions required for murine head morphogenesis. Together with previous studies, this work provides more conclusive evidence indicating that this control may play a central role in development and evolution of the vertebrate head.

MATERIALS AND METHODS

Targeting vectors, ES cell transfection and selection of targeted clones

The gene replacement vectors were generated from the same plasmid (pGN31) used to produce $Otx2^{-/-}$ mice (Acampora et al., 1995). For the otd^{2} construct, a *Bsu*36I/*Xmn*I fragment of the *otd* cDNA containing 56 bp of its 5′ UTR, the entire coding sequence and 450 bp of its 3′UTR was cloned in place of the *lacZ* gene in the former targeting vector. In this molecule, the *otd* cDNA was fused to the *Otx2* 5′UTR lacking 213 bp in front of the methionine.

For the otd^{2FL} allele, a chimeric fragment containing the 213 bp of the *Otx2* 5′UTR (missing in the otd^{2} locus), the *otd* coding sequence and the *Otx2* 3′UTR from the stop codon up to a sequence 57 bp upstream of the *Otx2* polyadenylation signal, was generated by PCR, sequenced and cloned in the same targeting vector. The control $Otx2^{2c}$ locus was generated using the same criteria as for otd^{2FL}, the *Otx2* cDNA coding sequence being the only difference. To facilitate both genotyping and molecular analysis, the *Otx2* cDNA was a chimeric fragment made up of human sequences from the methionine to the *Nsi*I site in exon 3 (Fig. 6A). Downstream of their 3′ UTR, all of the three molecules carried a SV40 polyadenylation signal to ensure transcription termination. The three targeting vectors were all electroporated into HM-1 embryonic stem cells. Homologous recombinant clones were identified by PCR using the same primers and conditions previously described (Acampora et al., 1995) (black arrows in Fig. 1A and Fig. 6A) and confirmed by hybridising *Hin*dIII digested genomic DNA with probes c and f (Fig. 1A,B, Fig. 6A,B and data not shown). Once established, all the mutant lines were kept in the B6D2 F1 genetic background.

Mouse genotyping

Genotyping was performed by PCR using two primers specific for the wild-type allele that were common for all the mouse lines (black arrowheads in Fig. 1A and 6A) (sense primer, GTGACTGAGAA-ACTGCTCCC; antisense primer, GTGTCTACATCTGCCCTACC) and three different pairs of primers for each mutated allele, *otd*^{2} (open arrowheads in Fig. 1A) (sense primer, ATCAAGACGCACCAC-AGTTCCT; antisense primer, TCCTTTAGCTGATCATAGGGCG), *otd*^{2FL} (open arrows in Fig. 1A) (sense primer, CTTCTGGCACA-ATCAGTACCAGC; antisense primer, TGCTGGTTGATGGAC-CCTTC) and *Otx2*^{2c} (open arrowheads in Fig. 6A) (sense primer, TCACTCGGGCGCAGCTAGATGTG; antisense primer, AGAGGA-GGTGGACAAGGGATCT). These primers amplify a 223 bp wild-type fragment and 444, 429 and 371 bp long fragments corresponding to the *otd*^{2}, *otd*^{2FL} and *Otx2*^{2c} mutant alleles, respectively (Fig. 1C and Fig. 6C).

RNAse protection assay

RNAse protection was performed as previously described (Simeone et al., 1993) using as probes, three fragments generated by PCR in corresponding regions (hatched boxes b, d in Fig. 1A and g in Fig. 6A). Phosphorimager scanning was performed to quantify RNA levels.

Immunohistochemistry and western blot analysis

Embryos were processed for immunohistochemistry with αOTD (1:1000) and αOTX2 (1:1500) polyclonal antisera as previously described (Acampora et al., 1998b). The αOTD polyclonal antiserum was generated following the same procedure previously used for the αOTX2 antiserum (Briata et al., 1996). Total extracts were prepared from three independent pools of 10.5 and 7.5 d.p.c. embryos for each mutant, processed for standard western blot assay and probed with αOTD (1:5000) and αOTX2 antiserum (1:5000). Films were processed for densitometric scanning.

In situ hybridisation and probes

In situ hybridisation experiments on sections and whole embryos were performed as previously described (Hogan et al., 1994; Simeone, 1999).

Wnt1, Tbr1, Bf1, Fgf8, Six3, Gbx2, Nog, Chd, cer-l, Hesx1 and

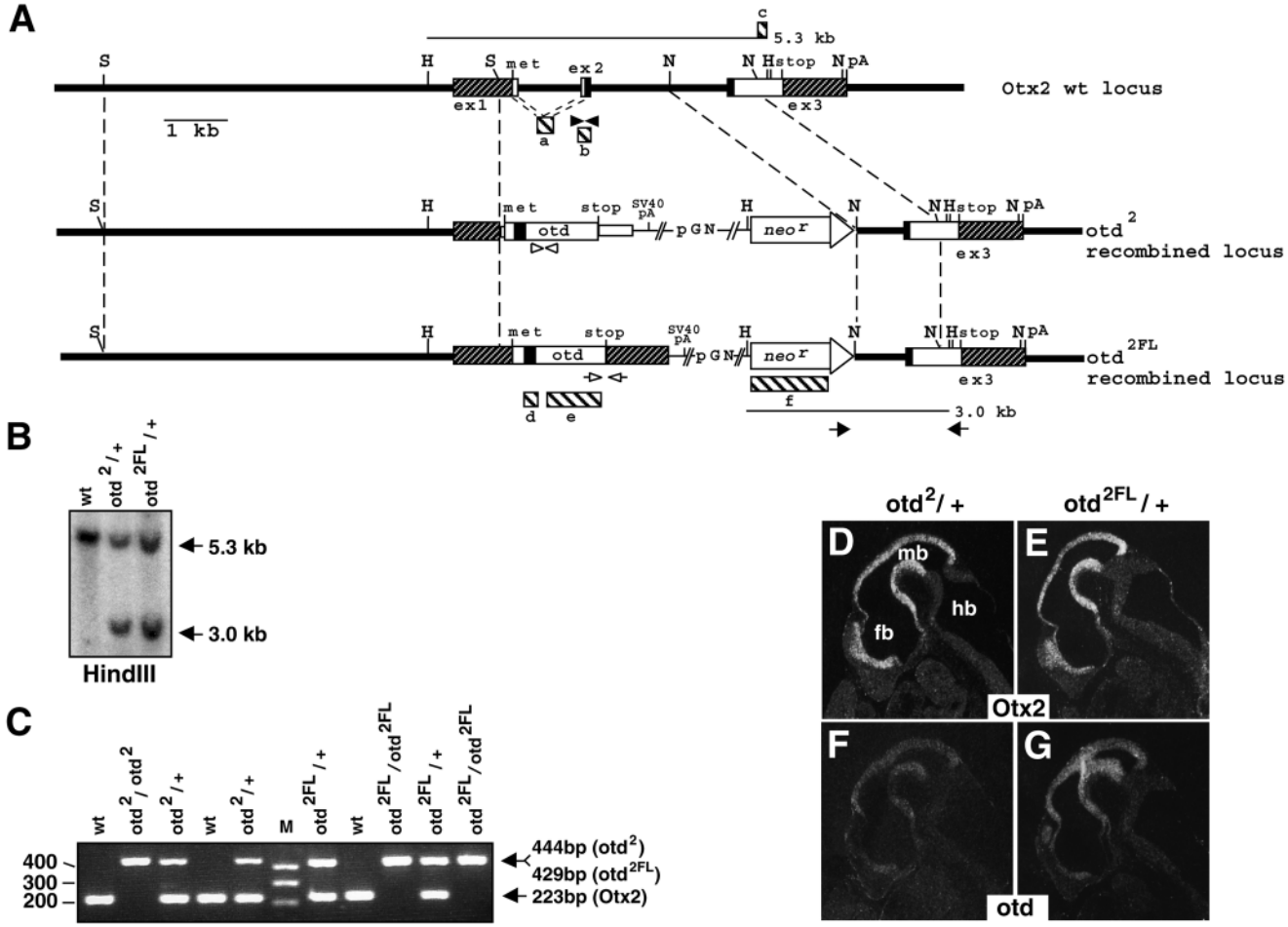

Fig. 1. Genomic organisation of the *otd*^{2} and *otd*^{2FL} targeted loci (A). The targeted loci are shown in the third and fourth line; first and last lines show *Hin*dIII fragments (5.3 and 3.0 kb) detected by southern blot analysis using probes (hatched boxes) external to the targeting vector (probe c) or within the *neomycin* gene (probe f). S, *Sma*I; H, *Hin*dIII; N, *Nsi*I; met, methionine; stop, stop codon; pA, polyadenylation signal. Dark hatched rectangles represent *Otx2* 5′ and 3′ UTRs, thinner open rectangles *Drosophila otd* UTRs. (B) Southern blot analysis of one representative targeted cell line for both molecules and wild-type HM-1 ES cells hybridised with probe c (see A). (C) PCR genotyping of two litters from two heterozygotes using the primers indicated in A as filled arrowheads (wild-type allele), open arrowheads (*otd*^{2} allele) and open arrows (*otd*^{2FL} allele). (D-G) In situ hybridisation of an *otd*^{2}/+ and an *otd*^{2FL}/+ embryo at 10.5 d.p.c. with *Otx2* (D,E) and *otd*-specific probes (probe a and e in A; F,G). fb, forebrain; mb, midbrain; hb, hindbrain.

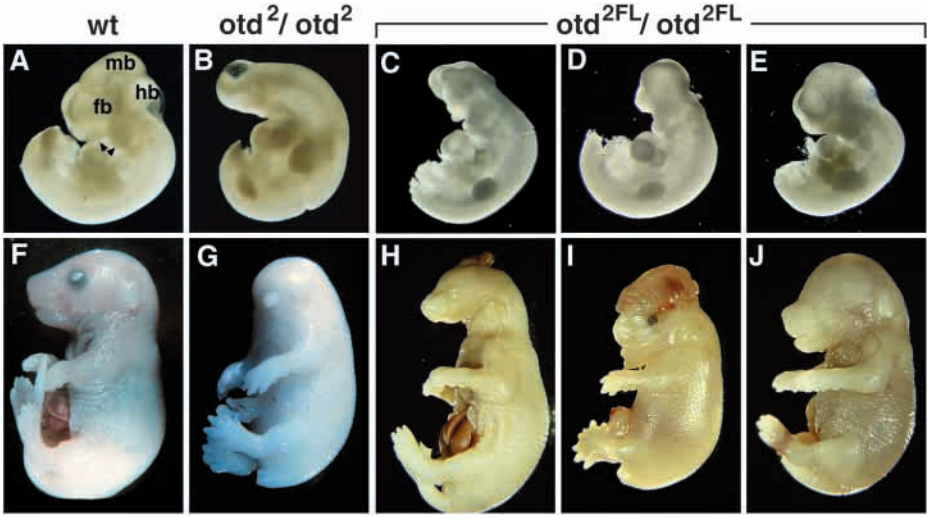

Fig. 2. Morphology of *otd²/otd²* and *otd^2FL/otd^2FL* embryos. (A-J) Compared to 10.5 and 16 d.p.c. wild-type embryos (A,F), *otd²/otd²* mutants exhibits a headless phenotype and normal body axis (B,G); while *otd^2FL/otd^2FL* embryos at 10.5 d.p.c. were classified on the basis of head abnormalities as severe (C), moderate (D,H,I) and mild (E,J). Abbreviations as in the previous figure.

Lim1 probes are the same previously described (Acampora et al., 1997; Acampora et al., 1998b; Pilo Boyl et al., 2001). The *otd* probe (probe e in Fig. 1A and Fig. 6A) is a PCR fragment spanning the last 800 bp of the *otd* coding region. The *Otx2* probe for in situ hybridisation on sections corresponds to probe a in Fig. 1A. The *Otx2^2c*-specific probe for in situ hybridisation experiments on sections corresponds to probe h in Fig. 6A.

Polysome gradients and RNA purification

Sucrose gradients were performed essentially as described (Loreni and Amaldi, 1992; Pilo Boyl et al., 2001). Nuclear and cytoplasmic mRNAs were purified as previously described (Pilo Boyl et al., 2001). Stability of *Otx2*, *otd²*, *otd^2FL* and *Otx2^2c* mRNAs was determined by administering 15 μg/ml of actinomycin D to the heterozygous ES cell clones followed by RNA extraction at the time indicated in Fig. 8F.

RESULTS

Generation of mice replacing *Otx2* with two *otd* cDNA carrying different 5′ and 3′ UTRs

In order to assess whether OTD is equivalent to OTX2 and whether this equivalence is subordinated to the *Otx2* post-transcriptional control, we generated two different mouse models replacing *Otx2* with *otd*.

In the first mutant locus (*otd²*) an *otd* cDNA containing 56 bp of the 5′ UTR, the full coding sequence, and 450 bp of the 3′ UTR region was introduced into an *Otx2* disrupted locus and fused at its 5′ end to the *Otx2* 5′ UTR and at its 3′ end to the SV40 poly(A) cassette of the pGN targeting vector (Acampora et al., 1995) (Fig. 1A). *Otx2* deleted or misplaced sequences included 213 bp upstream of the start methionine in the 5′ UTR, exons, introns and 3′ UTR (Fig. 1A).

In the second mutant locus (*otd^2FL*) the entire *Otx2*-5′ UTR and the *Otx2*-3′ UTR, excluding only the last 57 bp upstream of the polyadenylation signal, were fused to the methionine and stop codon of the *otd* coding sequence, respectively (Fig. 1A). The resulting heterozygotes (*otd²*/+ and *otd^2FL*/+) were healthy and fertile. Expression of the two mutated alleles was monitored in heterozygous embryos at 6.5 and 10.5 days post coitum (d.p.c.) by using *Otx2* and *otd* allele-specific probes (probes a and e in Fig. 1A). At 10.5 d.p.c. the *Otx2* (Fig. 1D,E), *otd²* (Fig. 1F) and *otd^2FL* (Fig. 1G) transcripts were properly co-expressed along the forebrain and midbrain of *otd²*/+ and *otd^2FL*/+ embryos, even though the amount of *otd²* transcripts appeared heavily reduced in *otd²*/+ embryos.

Similar experiments performed at 6.5 d.p.c., revealed that during gastrulation the amount of *otd²* mRNA was higher (Fig. 3 and Fig. 8).

Head abnormalities in *otd²/otd²* and *otd^2FL/otd^2FL* embryos

All *otd²/otd²* embryos at 10.5 d.p.c. (23 out of 23) had a striking headless phenotype (Table 1; Fig. 2B); approximately one third of them (7 out of 23) also had a reduced body size. Moreover in *otd²/otd²* mutants, the maxillary process, the mandibular arch and their derivatives were strongly impaired or absent (Fig. 2B,G).

In contrast, *otd^2FL/otd^2FL* mutants exhibited an evident morphological rescue of the anterior defects observed in *otd²/otd²* embryos, even though, head and brain development still appeared compromised (Table 1; Fig. 2C-E,H-J). Nevertheless, phenotype analysis (see also below) indicated that most of the *otd^2FL /otd^2FL* embryos (≥80%) exhibited forebrain and midbrain identities as well as ocular and olfactory sense organs (moderate and mild phenotypes in Table 1). Moderate phenotype was characterised by exencephaly and forebrain reduction (Fig. 2D,H,I); mild phenotype by a variable anterior shift of the presumptive midbrain-hindbrain boundary (MHB), and a well developed forebrain and anterior sense organs (Fig. 2E,J). Only a residual fraction (approx. 15%) of *otd^2FL/otd^2FL* embryos exhibited a severe phenotype (Table 1;

Table 1. Head abnormalities in *otd²/otd²* and *otd^2FL/otd^2FL* embryos at 10.5 d.p.c.

Genotype*	Phenotypes				Embryos scored
	Headless	Severe	Moderate	Mild	
otd²/otd²	23 (100%)‡	0	0	0	23
otd^2FL/otd^2FL	1 (3.5%)	4 (14%)	13 (46%)	10 (35%)	28

*The frequency of *otd²/otd²* and *otd^2FL/otd^2FL* genotypes at 10.5 d.p.c. was 17% and 22%, respectively.

‡7 out of 23 embryos also showed reduction in body size.

Fig. 2C). However, also these embryos showed midbrain-specific and, occasionally, forebrain-specific gene expression (data not shown). Only 1 out of the 28 otd^{2FL}/otd^{2FL} embryos scored, displayed a headless phenotype (Table 1).

These data suggest that, despite the huge diversity between the *Drosophila* OTD and the murine OTX2, the fly protein was able to compensate OTX2 functions that are required for head development.

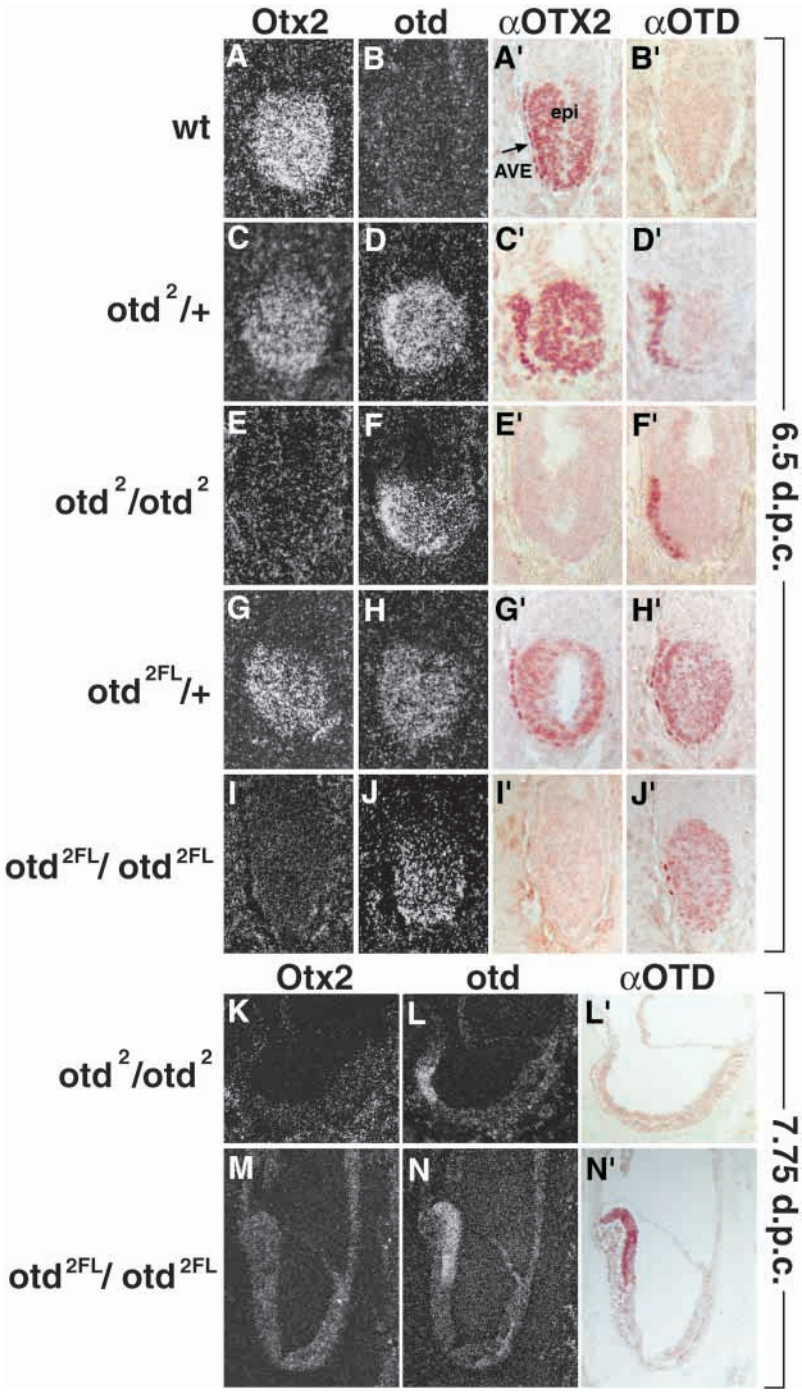

Fig. 3. Distribution of otd^2, otd^{2FL} and *Otx2* mRNAs and proteins during gastrulation. (A-N') Adjacent sagittal sections of 6.5 and 7.75 d.p.c. wild-type (A,B,A',B'), $otd^2/+$ (C,D,C',D') otd^2/otd^2 (E,F,E',F',K,L,L'), $otd^{2FL}/+$ (G,H,G',H') and otd^{2FL}/otd^{2FL} (I,J,I',J',M,N,N') embryos hybridised with probes specific for *Otx2* (A,C,E,G,I,K,M) and *otd* (B,D,F,H,J,L,N) mRNAs or immunostained with αOTX2 (A',C',E',G',I') and αOTD (B',D',F',H',J',L',N') antibodies. Abbreviations: AVE, anterior visceral endoderm; epi, epiblast.

Epiblast and neuroectoderm synthesis of OTD requires *Otx2* 5′ and 3′ UTR sequences

The phenotype of otd^2/otd^2 embryos revealed striking similarity with that of mice in which exactly the same *Otx2* region had been replaced with a human *Otx1* cDNA ($hOtx1^2$) (Acampora et al., 1998b). In this mutant, the *hOtx1* mRNA was transcribed in the VE and epiblast but translated only in the VE. Therefore transcription and translation was studied in otd^2 and otd^{2FL} mutants. A detailed analysis of otd^2 and otd^{2FL} mRNAs and proteins was performed at early streak (6.5 d.p.c.) and late streak (7.75 d.p.c.) stages in wild-type, $otd^2/+$, otd^2/otd^2, $otd^{2FL}/+$ and otd^{2FL}/otd^{2FL} embryos (Fig. 3). Genotypes were determined by hybridising adjacent sections with *Otx2* and *otd* allele-specific probes (probe a and e in Fig. 1A, respectively). Two additional series of adjacent sections were assayed for the presence of OTX2 and OTD proteins with αOTX2 and αOTD antibodies. No staining was detected with either of the two antibodies on $Otx2^{-/-}$ embryos (data not shown) (Acampora et al., 1998b).

Otx2 transcripts and protein distribution fully colocalised in the epiblast and VE of wild-type (Fig. 3A,A'), $otd^2/+$ (Fig. 3C,C') and $otd^{2FL}/+$ (Fig. 3G,G') embryos at 6.5 d.p.c. and similar results were obtained at 7.75 d.p.c. (data not shown).

In $otd^2/+$ and otd^2/otd^2 embryos, otd^2 transcripts were detected in VE and epiblast at 6.5 d.p.c. (Fig. 3D,F) and in the anterior neuroectoderm and ame at 7.75 d.p.c. (Fig. 3L and data not shown). Also, as previously mentioned, their amount did not differ greatly from that of the *Otx2* mRNA. In contrast with the otd^2 mRNA distribution in both VE and epiblast, at 6.5 d.p.c. the OTD protein appeared restricted to the VE of $otd^2/+$ (Fig. 3D') and otd^2/otd^2 (Fig. 3F') embryos and was not evident in the epiblast. Also at 7.75 d.p.c., OTD was not detected (Fig. 3L').

Importantly, in $otd^{2FL}/+$ and otd^{2FL}/otd^{2FL} embryos, both otd^{2FL} mRNA and protein colocalised in the VE and epiblast at 6.5 d.p.c. (Fig. 3H,H',J,J') as well as in the neuroectoderm and ame at 7.75 d.p.c. (Fig. 3N,N' and data not shown).

These data provide in vivo evidence that *Otx2* 5′ and 3′ UTRs are required for translation of the *Otx2* mRNA in epiblast and derived tissues. Moreover, the finding that the otd^2 mRNA is not translated in the epiblast of $otd^2/+$ embryos suggests that this control does not require OTX2.

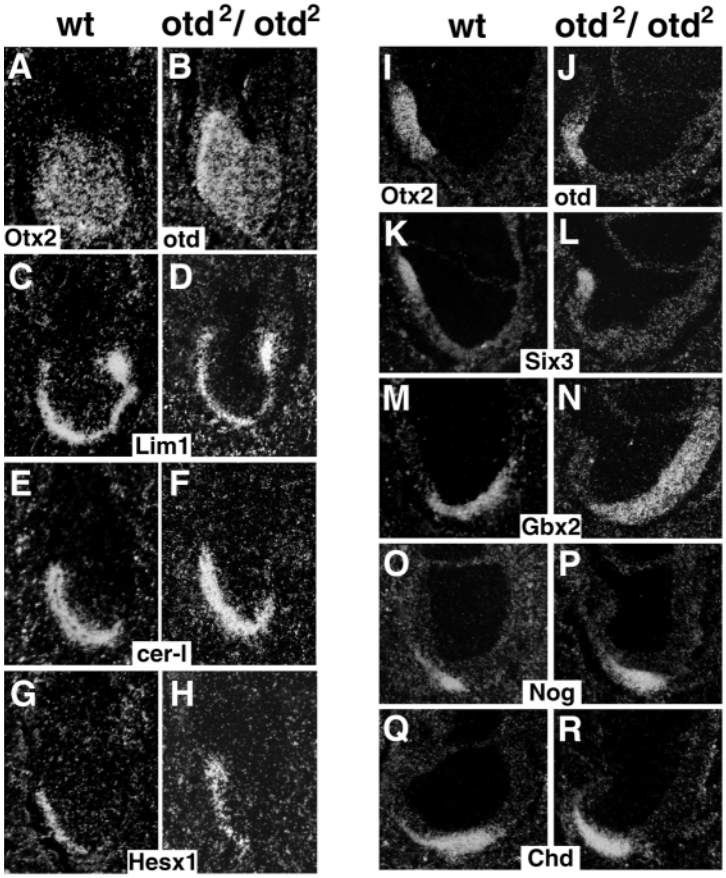

Fig. 4. Normal gastrulation and early anterior patterning in *otd²/otd²* embryos. (A-R) Sagittal sections of 6.5 d.p.c. (A-H) and 7.5 d.p.c. (I-R) wild-type (A,C,E,G,I,K,M,O,Q) and *otd²/otd²* (B,D,F,H,J,L,N,P,R) embryos hybridised with *Otx2* (A,I), *otd* (B,J), *Lim1* (C,D), *cer-l* (E,F), *Hesx1* (G,H), *Six3* (K,L), *Gbx2* (M,N), *Nog* (O,P) and *Chd* (Q,R).

Nevertheless, on the basis of these data it cannot be excluded whether this control requires both *Otx2* coding sequence and 5′ and 3′ UTRs in a *cis* configuration.

otd²/otd² and *otd^2FL/otd^2FL* embryos rescue *Otx2* requirement in the VE and exhibit normal patterning of the early neural plate

Previous data indicated that the earliest defects of *Otx2*$^{-/-}$ embryos are related to an OTX2 requirement in the VE that is abnormally located at the distal tip of the embryo as revealed by the expression of *Lim1*, *cerberus-like (cer-l)*, *Hesx1* (Acampora et al., 1995; Acampora et al., 1998b; Ang et al., 1996). To assess whether the OTD protein could rescue these impairments, *otd²/otd²* embryos were studied at 6.5 and 7.5 d.p.c. In *otd²/otd²* embryos, *otd²* mRNA was detected in the VE and epiblast (Fig. 4B) and *Lim1*, *cer-l* and *Hesx1* were correctly expressed (Fig. 4D,F,H).

Therefore, VE abnormalities and molecular impairments detected in *Otx2*$^{-/-}$ embryos were rescued by the VE-restricted translation of the *otd²* mRNA. This suggests that OTD and OTX2 proteins exhibit functional equivalence in the VE.

At late streak-headfold stage, *Otx2*$^{-/-}$ embryos were severely impaired in morphology and expression of early forebrain, midbrain and hindbrain markers (Acampora et al., 1995; Acampora et al., 1998b; Matsuo et al., 1995; Ang et al., 1996; Rhinn et al., 1998). In *otd²/otd²* embryos, *otd²* transcripts were restricted to the presumptive forebrain and midbrain (Fig. 4J), *Six3* was expressed in the rostralmost neuroectoderm (Fig. 4L) and *Gbx2* throughout the presumptive hindbrain (Fig. 4N).

Otx2 null embryos also showed severe impairments of the gastrulation process. Accordingly, *Noggin (Nog)* and *Chordin (Chd)* transcripts were either absent or only barely detected in disorganised cells (Acampora et al., 1995; Acampora et al., 1998b; Ang et al., 1996). As revealed by *Nog* (Fig. 4P) and *Chd* (Fig. 4R) expression, these defects were recovered in *otd²/otd²* embryos. This analysis was also performed in 6.5 and 7.5 d.p.c. *otd^2FL/otd^2FL* embryos which, as expected, did not show any abnormalities (data not shown).

Thus, the morphological defects and the molecular impairments that affect VE, rostral neuroectoderm, primitive streak, as well as the node and its derivatives of *Otx2*$^{-/-}$ embryos are rescued by VE-restricted translation of *otd²* mRNA. It is noteworthy that the additional presence of OTD protein in the epiblast of *otd^2FL/otd^2FL* embryos does not improve the rescue observed when the OTD protein is restricted to the VE. This strengthens the idea that in *Otx2*$^{-/-}$ embryos, *Otx2*-mediated impairments of the early anterior patterning and primitive streak are determined in the VE.

Maintenance of anterior patterning is rescued in *otd^2FL/otd^2FL* embryos

We previously showed that *hOtx1²/hOtx1²* embryos failed to maintain anterior patterning and exhibited headless phenotype (Acampora et al., 1998b).

Embryo morphology and lack of OTD protein in epiblast and neuroectoderm are very similar in *otd²/otd²* and *hOtx1²/hOtx1²* embryos. On this basis, maintenance of forebrain and midbrain identity should be lost in *otd²/otd²* mutants. To assess this issue, the expression of a number of regionally restricted markers such as *Fgf8*, *Gbx2*, *Wnt1*, *Bf1* and *Tbrain1* (*Tbr1*) was analysed together with *otd* at 8.5 and 10.5 d.p.c.

Compared to wild-type embryos (Fig. 5A-J), in *otd²/otd²* embryos at 8.5 and 10.5 d.p.c., *otd²* transcripts were undetectable along the neuroectoderm (Fig. 5A'); *Fgf8* (Fig. 5B',G'), *Gbx2* (Fig. 5C') and *Wnt1* (Fig. 5D',H') expression was markedly displaced anteriorly; *Bf1* (Fig. 5E',I') and *Tbr1* (Fig. 5J') were no longer detected in presumptive forebrain. In *otd^2FL/otd^2FL* embryos recovery of forebrain and midbrain regional identity was observed.

Indeed, compared to *otd²/otd²* embryos, *otd^2FL* expression was detected and maintained along the anterior neural plate (Fig. 5A'',F''); *Fgf8* (Fig. 5B'') and *Gbx2* (Fig. 5C'') expression domains were shifted posteriorly almost at their normal position; *Wnt1* (Fig. 5D'') transcripts were detected in a broader domain corresponding to the presumptive midbrain; *Bf1* (Fig. 5E'',I'') was abundant in the rostral neuroectoderm, and *Tbr1* (arrow in Fig. 5J''), which labelled post-mitotic neuroblasts in the dorsal telencephalon, was properly expressed.

However, even though the forebrain and midbrain rescue determined by the fly OTD protein was evident in most of *otd^2FL/otd^2FL* mutants, it was never complete. Indeed, at 10.5

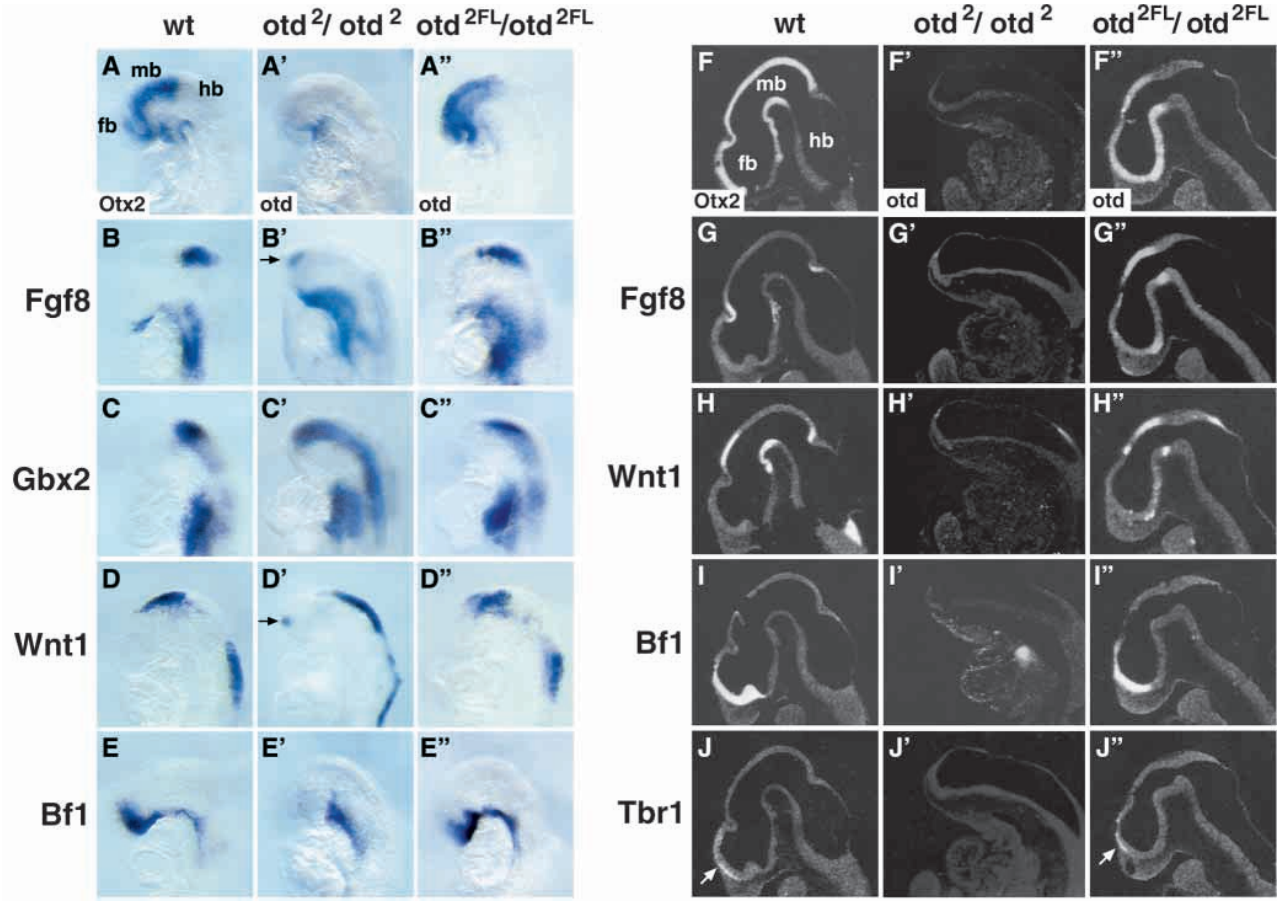

Fig. 5. Lack of forebrain and midbrain identities in the *otd*^{2}/*otd*^{2} mutant is rescued in *otd*^{2FL}/*otd*^{2FL} embryos. (A-E'') Whole-mount in situ hybridisation of 8.5 d.p.c. wild-type (A-E), *otd*^{2}/*otd*^{2} (A'-E') and *otd*^{2FL}/*otd*^{2FL} (A''-E'') embryos with *Otx2* (A) *otd* (A',A''), *Fgf8* (B,B',B''), *Gbx2* (C,C',C''), *Wnt1* (D,D',D'') and *Bf1* (E,E',E''). (F-J'') Adjacent sagittal sections of 10.5 d.p.c. wild-type (F-J), *otd*^{2}/*otd*^{2} (F'-J') and *otd*^{2FL}/*otd*^{2FL} (F''-J'') embryos hybridised with *Otx2* (F), *otd* (F',F''), *Fgf8* (G,G',G''), *Wnt1* (H,H',H''), *Bf1* (I,I',I'') and *Tbr1* (J,J',J''). Abbreviations as in previous figures.

d.p.c. the midbrain territory defined by *otd*^{2FL} and *Wnt1* expression domains (Fig. 5F'',H'') was smaller and this reduction was balanced by an enlargement of the rostalmost hindbrain. Moreover, *Fgf8* (Fig. 5G'') expression was abnormally expanded within the *otd*^{2FL} and *Wnt1* domains.

Finally, it is noteworthy that all the embryos with a moderate phenotype (Table 1 and Fig. 2D) recovered forebrain and midbrain expression of *Bf1*, *Tbr1*, *Wnt1* and *otd*^{2FL} (data not shown) and that 3 out of 6 embryos with a severe phenotype (Table 1 and Fig. 2C) exhibited spotted expression of *Bf1* (data not shown).

Therefore, this analysis indicates that (i) the *Drosophila* OTD and the murine OTX2 proteins share functional equivalence also in the neural plate where OTD is able to maintain the anterior patterning and direct forebrain and midbrain regionalisation; and (ii) OTD/OTX2 equivalence in maintenance of forebrain and midbrain depends on the translation of the *otd*^{2FL} mRNA in the epiblast and neural plate and this process requires *Otx2* 5′ and 3′ UTRs.

Embryos replacing *Otx2* with an *Otx2* cDNA (*Otx2*^{2c}/*Otx2*^{2c}) display the same phenotype exhibited by *otd*^{2FL}/*otd*^{2FL} mutants

The phenotypic features of *otd*^{2FL}/*otd*^{2FL} embryos are reminiscent of those previously described in mutant embryos with reduced level of OTX2 or both OTX2 and OTX1 proteins (Acampora et al., 1997; Suda et al., 1997; Pilo Boyl et al., 2001). This suggests that the level of OTD protein is not sufficient to fulfil all of the OTX2 requirements. Alternatively, it may suggest that OTD and OTX2 proteins share partial functional equivalence.

To address this issue, we have generated a third mouse model replacing *Otx2* with an *Otx2* cDNA (*Otx2*^{2c}) with the same strategy used to generate the *otd*^{2FL} recombined locus (compare Fig. 6A with Fig. 1A). The *Otx2*^{2c} recombined locus was therefore identical to the *otd*^{2FL} locus, except for the *Otx2* coding sequence and, thereby, it should represent the most appropriate control of the *otd*^{2FL} mutated locus.

Otx2^{2c}/*Otx2*^{2c} and *otd*^{2FL}/*otd*^{2FL} embryos exhibited striking phenotypic similarities. Indeed, also *Otx2*^{2c}/*Otx2*^{2c} embryos were classified in three groups on the basis of head abnormalities (Table 2) (Fig. 6E-G,I-K). At 7.5 d.p.c. *Otx2*^{2c} mRNA and protein colocalised in the anterior neuroectoderm and ame of *Otx2*^{2c}/*Otx2*^{2c} embryos (data not shown) and *Six3*, *Chd* and *Gbx2* were correctly expressed (data not shown). Maintenance of the anterior patterning was assessed at 8.5 and 10.5 d.p.c. by analysing the expression of *Otx2*^{2c}, *Fgf8*, *Gbx2* and *Bf1* as well as the distribution of the OTX2 protein. At 8.5

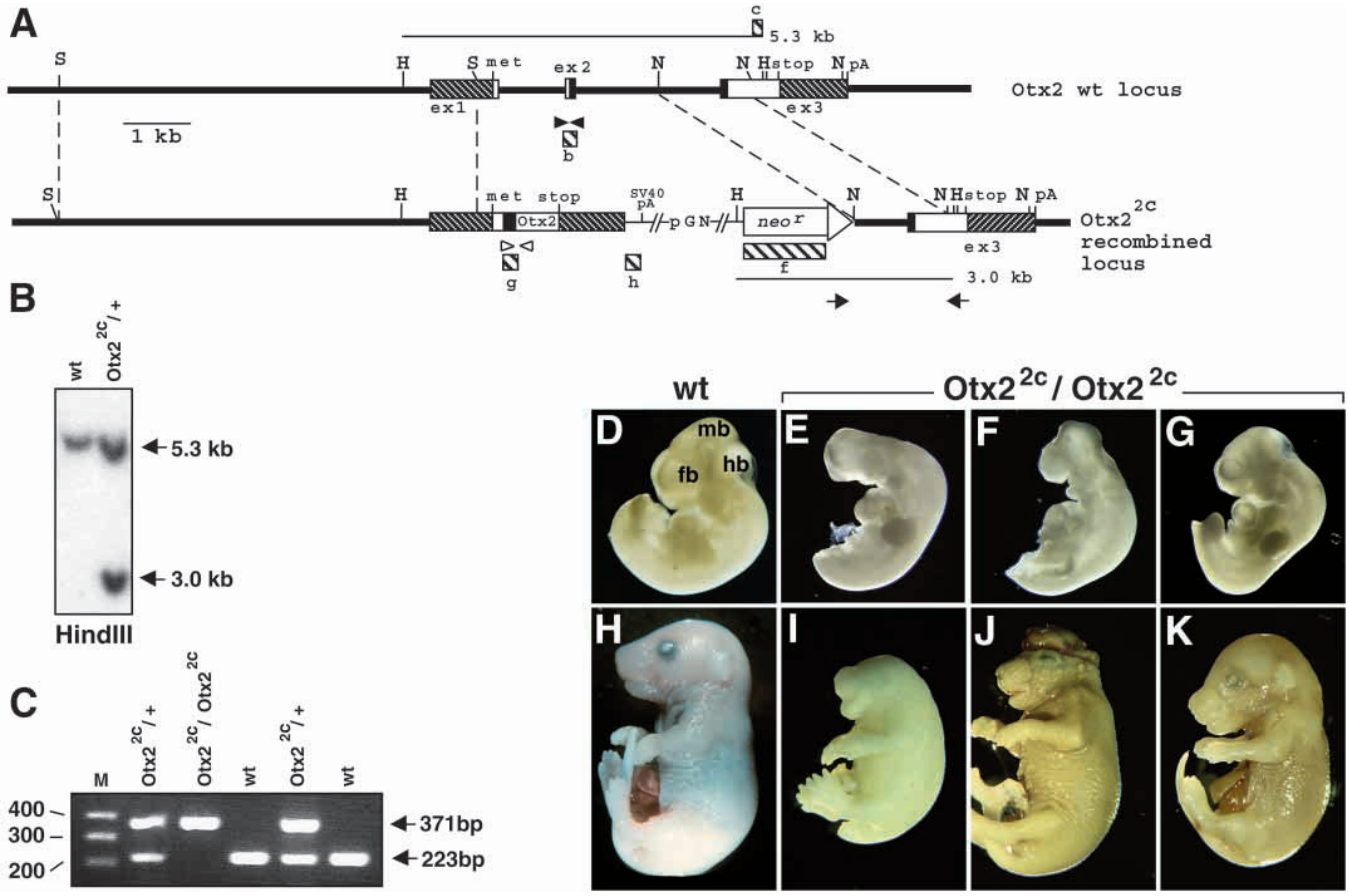

Fig. 6. Genomic organisation of the *Otx2*^{2c} targeted locus. (A) The targeted locus is shown in the third line; first and last lines show *Hin*dIII fragments (5.3 and 3.0 kb) detected by Southern blot using the same probes (hatched boxes c and f) as in Fig. 1A. Abbreviations are as in legend to Fig. 1. (B) Southern blot analysis of one representative targeted cell line and wild-type HM-1 ES cells hybridised with probe c (see A). (C) PCR genotyping of a litter from two heterozygotes using the primers indicated in (A) as filled arrowheads (wild-type allele) and open arrowheads (*Otx2*^{2c} allele). (D-K) Compared to 10.5 and 16 d.p.c. wild-type embryos (D,H), *Otx2*^{2c}/*Otx2*^{2c} (E-G,I-K) phenotypes were classified on the basis of head abnormalities as severe (E,I), moderate (F,J) and mild (G,K). Note the similarity between *Otx2*^{2c}/*Otx2*^{2c} and *otd*^{2FL}/*otd*^{2FL} (Fig. 2) phenotypes. Abbreviations as in previous figures.

d.p.c., *Otx2*^{2c}/*Otx2*^{2c} embryos showed that *Otx2*^{2c} was transcribed along the presumptive forebrain and midbrain (Fig. 7A'), and *Fgf8* (Fig. 7B') and *Gbx2* (Fig. 7C') expression domains appeared slightly expanded anteriorly. At 10.5 d.p.c. in *Otx2*^{2c}/*Otx2*^{2c} embryos, *Otx2*^{2c} transcripts (data not shown) and protein (Fig. 7E') colocalised and were less abundant in the posterior midbrain; *Fgf8* (Fig. 7F') was broadly expressed up to the presumptive position of the telen-diencephalic boundary; *Gbx2* transcripts (Fig. 7G') were slightly displaced anteriorly and a robust expression of *Bf1* (Fig. 7D',H') was detected in the forebrain at 8.5 and 10.5 d.p.c.

Therefore, these findings and those reported for *otd*^{2FL}/*otd*^{2FL} embryos suggest that OTD and OTX2 functional properties may be fully equivalent. However, from our data it cannot be excluded that OTD is unable to fully rescue the *Otx2* mutant phenotype when only the *Otx2* coding sequence is replaced.

Otx2 5′ and 3′ UTRs are required for nucleo-cytoplasmic export and epiblast-restricted translation of *Otx2* mRNA

In order to determine the molecular events that were impaired in *otd*^{2}/*otd*^{2}, *otd*^{2FL}/*otd*^{2FL} and *Otx2*^{2c}/*Otx2*^{2c} embryos as well as those that were rescued by the presence of the *Otx2* 5′ and 3′ UTRs, a detailed analysis was performed to assess protein levels and to determine whether *otd*^{2}, *otd*^{2FL} and *Otx2*^{2c} mRNAs were efficiently transcribed, processed and translated. Protein levels were assessed in western blot assays on three independent pools of wt, *Otx2*$^{+/-}$, *otd*^{2}/+, *otd*^{2FL}/+ and *Otx2*^{2c}/*Otx2*^{2c} embryos at 7.5 and 10.5 d.p.c. At 7.5 d.p.c. OTD protein was detected only in *otd*^{2FL}/+ embryos (Fig. 8A) and its quantification indicated that, it was only 27% that of OTX2. A very similar result was obtained at 10.5 d.p.c. (data not shown). However, we were aware that the accuracy of this

Table 2. Head abnormalities in *Otx2*^{c}/*Otx2*^{c} embryos at 10.5 d.p.c.

	Phenotypes				
Genotype*	Headless	Severe	Moderate	Mild	Embryos scored
Otx2^{c}/*Otx2*^{c}	2 (4.7%)	9 (21.5%)	15 (36%)	16 (38%)	42

*The frequency of *Otx2*^{c}/*Otx2*^{c} genotype at 10.5 d.p.c. was 23%.

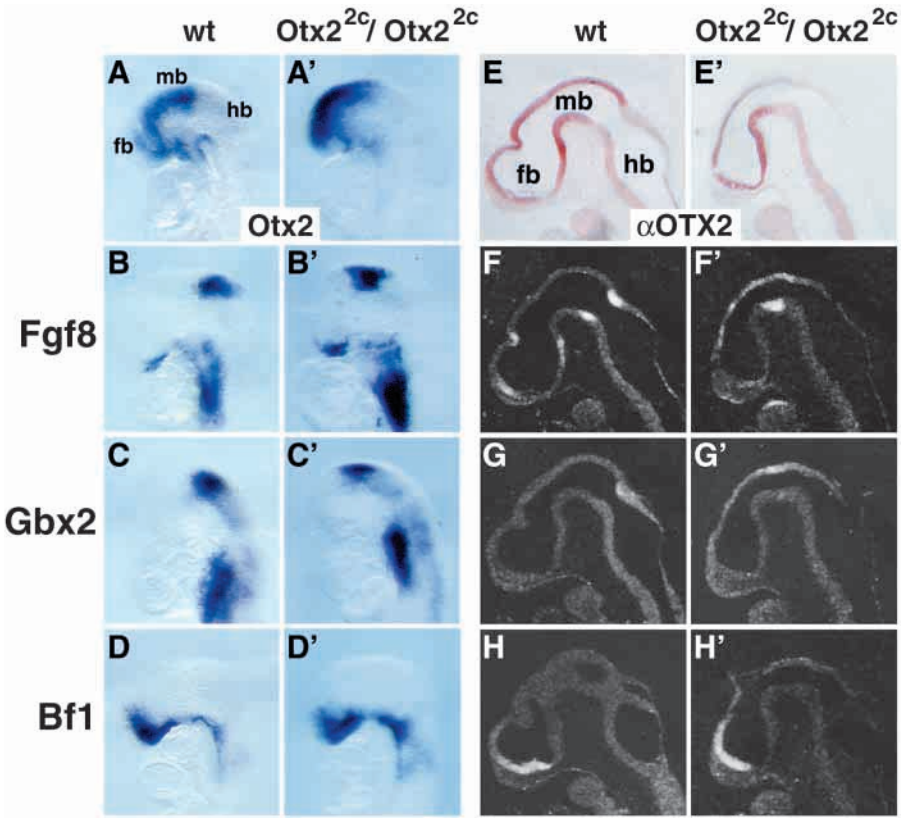

Fig. 7. *Otx2*^{2c}/*Otx2*^{2c} embryos exhibit similarities with *otd*^{2FL}/*otd*^{2FL} embryos in forebrain and midbrain patterning. (A-D') Whole-mount in situ hybridisation of 8.5 d.p.c. wild-type (A-D) and *Otx2*^{2c}/*Otx2*^{2c} (A'-D') embryos with *Otx2* (A,A'), *Fgf8* (B,B'), *Gbx2* (C,C') and *Bf1* (D,D'). (E-H') Adjacent sagittal sections of 10.5 d.p.c. wild-type (E-H) and *Otx2*^{2c}/*Otx2*^{2c} (E'-H') embryos, immunostained with αOTX2 (E,E') or hybridised with *Fgf8* (F,F'), *Gbx2* (G,G') and *Bf1* (H,H'). Abbreviations as in the previous figures.

quantitative analysis could be affected by different affinity and specificity of the two antibodies (αOTD and αOTX2), mainly in denaturing conditions. Indeed, based on αOTD and αOTX2 calibration experiments performed on HeLa cell extracts transfected with *Otx2*- and *otd*-expressing vectors and normalised for *Otx2* and *otd* mRNAs, we strongly suspected that the OTD level detected (27%) was underestimated (data not shown). This was also supported by the quantitative analysis performed in *Otx2*^{2c}/*Otx2*^{2c} embryos at 7.5 d.p.c. (Fig. 8B), which showed that the OTX2 level was 37% and 85% of that detected in wild-type and *Otx2*$^{+/-}$ embryos, respectively. Hence, this analysis confirms that head abnormalities observed in *otd*^{2FL} and *Otx2*^{2c} homozygous embryos are probably the consequence of a reduction in the amount of OTD and OTX2.

Next, we analysed whether *otd*^{2}, *otd*^{2FL} and *Otx2*^{2c} mRNAs were efficiently transcribed and processed. In order to compare wild-type and mutant mRNAs in the same cells, this analysis was performed in heterozygous embryos.

In these experiments, allele-specific probes (Fig. 1A, Fig. 6A) designed in the same region and of similar length were employed in order to minimise experimental heterogeneity. Compared to the *Otx2* mRNA, the cytoplasmic *otd*^{2} mRNA detected in 10.5 d.p.c. embryos was considerably diminished (14%), while at 7.5 d.p.c. it was remarkably higher (32%) (Fig. 8E). In contrast, the amount of the nuclear *otd*^{2} mRNA was abnormally high, being up to 50% that of the *Otx2* mRNA at 10.5 d.p.c and 90% at 7.5 d.p.c. (Fig. 8E).

The same analysis was performed in *otd*^{2FL}/+ and *Otx2*^{2c}/+ embryos at 10.5 d.p.c. In these mutants cytoplasmic and nuclear mRNA levels decreased by approximately 60% and 50%, respectively (Fig. 8E).

Hence, as nuclear and cytoplasmic mRNAs underwent a similar reduction, nucleo-cytoplasmic export and processing should be unaffected in these embryos. In contrast, the remarkable accumulation of the nuclear *otd*^{2} mRNA suggests that nucleo-cytoplasmic export is heavily affected. This implies that sequences within the *Otx2* 5′ and 3′ UTRs play a relevant role in this process.

In this context, the quantitative reduction observed in *otd*^{2FL}/+ and *Otx2*^{2c}/+ embryos should be ascribed to perturbation in transcription and/or stabilisation of the mutant mRNAs. Actinomycin D experiments performed on *otd*^{2}/+, *otd*^{2FL}/+ and *Otx2*^{2c}/+ ES cell lines indicated that the half-life of the mutant mRNAs was very similar to that of the *Otx2* mRNA ($t_{1/2}$=90 minutes) (Fig. 8F).

This suggests that lack of introns and insertion of the targeting vector may severely interfere with the transcription of the *Otx2* locus and, thereby, be responsible for the partial rescue observed in *otd*^{2FL}/*otd*^{2FL} and *Otx2*^{2c}/*Otx2*^{2c} embryos.

Finally, the ability of *otd*^{2}, *otd*^{2FL} and *Otx2*^{2c} mRNAs to form efficient polyribosome complexes was studied. Cytoplasmic extracts from 10.5 d.p.c. *otd*^{2}/+ heads were fractionated on a sucrose gradient and mRNA purified from each fraction. Distribution of *β-actin* and *Otx2* mRNAs along the gradient was analysed with the mutant mRNA. According to the length of β-actin (350 amino acids) and OTX2 (289 amino acids) coding sequences, ≥50% of their mRNAs was concentrated in the first two fractions that contained polyribosome complexes with >10 and 8-10 ribosomes (Fig. 9A,B). Similarly, the *otd*^{2} mRNA that encodes a 548 amino acid long protein should be concentrated in the fractions with the highest number of ribosomes, if efficiently translated. In contrast, approx. 60% of the *otd*^{2} mRNA was distributed among the central fractions of the gradient containing ≤5-7 ribosomes. This finding indicates that the *otd*^{2} mRNA is severely affected in its ability to form efficient polyribosome complexes.

The same experiment was performed on *otd*^{2FL}/+ and *Otx2*^{2c}/+ embryos (Fig. 9A,C,D). Importantly, in these embryos the *otd*^{2FL} (Fig. 9A,C) and the *Otx2*^{2c} (Fig. 9A,D) mRNAs were correctly distributed and ≥60% of the *otd*^{2FL} mRNA was concentrated in the first two fractions (Fig. 9C) and ≥60% of the *Otx2*^{2c} mRNA colocalised with the *Otx2* mRNA. This result provides direct in vivo evidence that the *Otx2* 5′ and

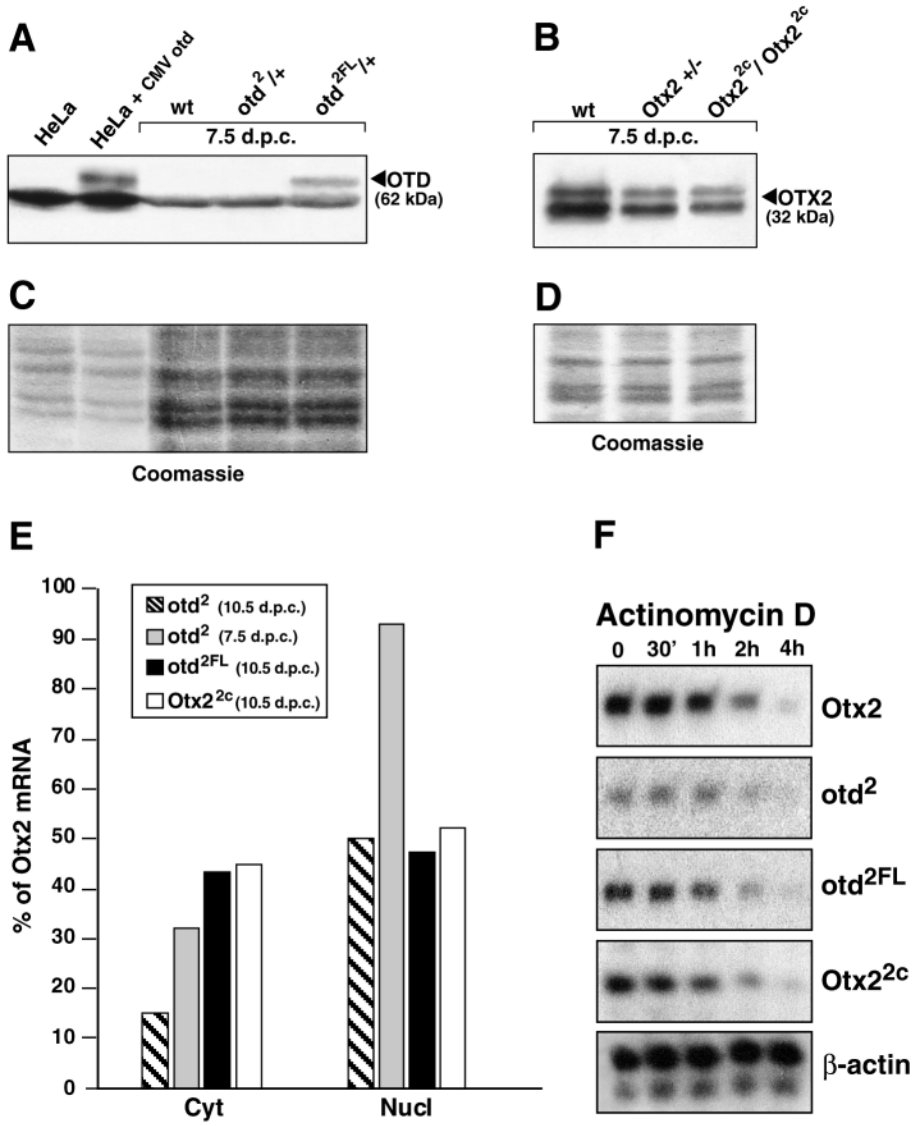

Fig. 8. Quantitative analysis of OTD and OTX2 proteins, *otd*^{2}, *otd*^{2FL} and *Otx2*^{2c} mRNAs and their stability in ES cells. (A) Western blot analysis of extracts from HeLa cells, HeLa cells transfected with an *otd*-expressing vector, and 7.5 d.p.c. wild-type, *otd*^{2}/+ and *otd*^{2FL}/+ embryos. (B) Western blot analysis on extracts from 7.5 d.p.c wild-type, *Otx2*$^{+/-}$ and *Otx2*^{2c}/*Otx2*^{2c} embryos. (C,D) Coomassie Blue staining of the gels in A and B. (E) *otd*^{2}, *otd*^{2FL} and *Otx2*^{2c} cytoplasmic and nuclear mRNA levels were determined in *otd*^{2}/+, *otd*^{2FL}/+ and *Otx2*^{2c}/+ embryos and are reported as percentages of the *Otx2* mRNA. *otd*^{2} mRNA was also analysed at 7.5 d.p.c. Note that while the *otd*^{2} cytoplasmic mRNA is considerably reduced, the *otd*^{2} nuclear mRNA has accumulated significantly. (F) Stability of *otd*^{2}, *otd*^{2FL} and *Otx2*^{2c} mRNA is comparable to that of *Otx2* mRNA in actinomycin D experiments performed on heterozygous ES cell lines.

3′ UTR sequences deleted in *otd*^{2} mutants are essential for both *otd*^{2FL} and *Otx2*^{2c} mRNAs to be correctly translated.

Distribution and quantitative mRNA analysis as well as translational efficiency were also studied in the *hOtx1*^{2} mutant. Indeed, also in this case lack of protein in the epiblast and its derivatives correlated with the deletion of the same *Otx2* 5′ and 3′ UTRs deleted in the *otd*^{2} mutant. In this mutant, the cytoplasmic *hOtx1* mRNA was approx. 40% of the *Otx2* mRNA, while the *hOtx1* nuclear mRNA accumulated up to approx. 140% of the *Otx2* nuclear mRNA (Fig. 9E). This indicates that impairment of nucleo-cytoplasmic export, identified in *otd*^{2} mutants, was also observed in *hOtx1*^{2} mutant embryos. The ability of the *hOtx1* mRNA to form polyribosome complexes was also greatly impaired and only ≤25% of its mRNA was detected in the first two fractions where, based on the length of the protein (355 amino acids), most of the *hOtx1* mRNA should be concentrated.

Therefore, also in the *hOtx1*^{2} mutant, heavy accumulation of nuclear mRNA and impairment in translation correlate as in the *otd*^{2} mutant, with lack of *Otx2* 5′ and 3′ UTRs. This molecular analysis has demonstrated by both gain- and loss-of-function experiments in four different mouse models that the *Otx2* 5′ and 3′ UTRs are crucial in controlling nucleo-cytoplasmic export and translation of the *Otx2* mRNA.

However, although these data cannot demonstrate whether the nucleo-cytoplasmic export is also affected only in the epiblast and neuroectoderm, they provide further support to the concept that murine brain development requires accurate epiblast-restricted translational control of the *Otx2* mRNA.

DISCUSSION

Until recently, it has been generally assumed that the insect and vertebrate CNS are non-homologous structures that evolved independently (Garstang, 1928; Lacalli, 1994).

For example, the so-called auricularia hypothesis postulates that the chordate CNS is homologous to the entire outer ectoderm of the insect embryo, based on both anatomical studies made in echinoderms (particularly auricularia larvae) and urochordates as well as on comparative expression of the HOX genes (Garstang, 1928; Lacalli, 1994). In contrast to such

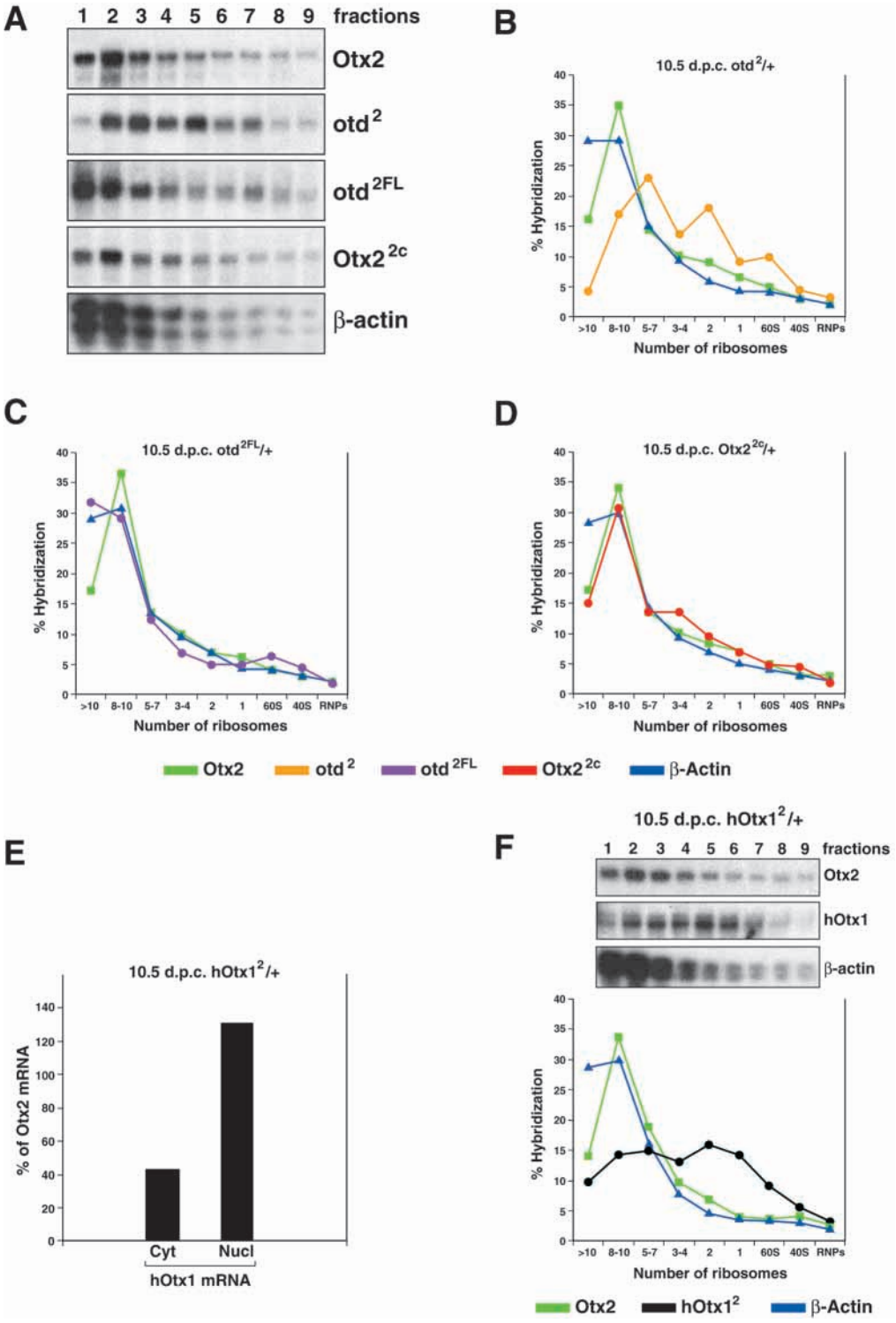

Fig. 9. *otd*^{2}, *otd*^{2FL}, *Otx2*^{2c} and *hOtx1* mRNAs form polyribosome complexes with different efficiencies. (A) RNAse protection experiments showing the distribution of *Otx2*, *otd*^{2}, *otd*^{2FL}, *Otx2*^{2c} and β-*actin* mRNAs along the fractions of polysome sucrose gradients. (B-D) Ribosome affinity profiles comparing the distribution of *Otx2* and β-*actin* mRNAs with that of *otd*^{2} (B), *otd*^{2FL} (C) and *Otx2*^{2c} (D) mRNAs. (E) Quantitative analysis of *hOtx1* cytoplasmic and nuclear mRNA showing a strong accumulation of nuclear RNA. (F) Ribosome affinity profile of the *hOtx1* mRNA indicates a severe impairment in forming efficient polyribosome complexes. Note that mRNA profiles are not influenced by any quantitative variation of the mRNA analysed.

hypotheses, and beginning with the highly debated proposal by Geoffroy Saint-Hilaire (Lacalli, 1994; Peterson, 1995; Arendt and Nübler-Jung, 1999), an increasing body of evidence has now accumulated that suggests a common evolutionary origin of the insect and vertebrate CNS (Arendt and Nübler-Jung, 1996, Arendt and Nübler-Jung, 1999; De Robertis and Sasai, 1996).

A growing number of molecular genetic studies support the idea of a common evolutionary origin of the CNS in different phyla. In *Drosophila* and vertebrates, the conserved families of HOM-C/HOX, *otd/Otx*, *empty spiracles (ems)/Emx* as well as *en/En* and *wingless (wg)/Wnt* genes play a fundamental role in the regional specification of the neuroectoderm destined to form nerve cord/posterior brain and anterior brain as well as in the establishment of boundary regions between them (Joyner, 1996; Lumsden and Krumlauf, 1996; Hanks et al., 1998; Araki and Nakamura, 1999; Reichert and Simeone, 1999).

Despite the overall morphological differences, expression pattern and mutant phenotypes for *Drosophila otd* and mouse *Otx* genes can have obvious parallels.

Nevertheless, OTD and OTX proteins are highly conserved only in the homeodomain, which represents roughly one-tenth of the whole OTD protein and about one-sixth and one-fifth of OTX1 and OTX2 proteins, respectively (Simeone et al., 1993). This suggests that *Otx* genes have either acquired new functions during evolution and these reside outside the homeodomain or, alternatively, that the functional properties of the non-homeodomain regions are common to both OTD and OTX but they are difficult to identify in the amino acid sequence. This study and previous reports (Acampora et al.,

1998a; Leuzinger et al., 1998; Nagao et al., 1998) indicate that, despite the restricted homology in their amino acid sequence, OTD/OTX proteins share a remarkable and unexpected functional equivalence in mice and flies.

Indeed, although an OTD-mediated rescue of OTX1 functions could be expected in neuronal cells (Acampora et al., 1998a), it is totally unexpected, in our opinion, that the fly gene is able to rescue OTX2-dependent properties that are encoded by the VE and neuroectoderm for early induction of the anterior patterning and maintenance of forebrain and midbrain regionalisation. It may suggest that even though OTD/OTX proteins have gained new role(s) during evolution, their basic properties have been retained. In this sense it is noteworthy that the absence of the lateral semicircular duct of the inner ear of *Otx1*$^{-/-}$ mice is never recovered either by *otd* or *Otx2*, thus indicating that the ability to specify this sensorial structure may, therefore, represent a new *Otx1*-specific property (Acampora et al., 1996; Acampora et al., 1998a; Acampora et al., 1999; Morsli et al., 1999). However, the molecular nature of functional equivalence between sequences outside the OTD/OTX homeodomain is still unclear and remains to be investigated in detail. Assuming that *otd* and *Otx2* gene functions are conserved, it is unclear why the brain vesicles of protochordates have been so deeply and suddenly modified in a much more complex brain that has been maintained in its basic topography until mammals. A rather obvious answer to this question is that new genetic functions have been recruited and stabilised, thus creating new versions of pre-existing developmental pathways (Acampora and Simeone, 1999; Holland 1999; Acampora et al., 2001). Indeed, it might be that conserved functions such as those encoded by OTD/OTX proteins become able to perform new roles even while retaining an evolutionary functional equivalence because they acquire the ability to be expressed in new cell types. Based on this hypothesis, it is expected that drastic evolutionary events should act on the regulatory control (transcription and translation) of *Otx*-related genes rather than on their coding sequences.

Here, we report that OTD is functionally equivalent to OTX2 only when the OTD encoding mRNA is provided with the 5′ and 3′ UTRs of *Otx2*. This implies that besides the *Otx2* transcriptional control, synthesis of OTD protein also requires the *Otx2* regulatory control for nucleo-cytoplasmic export and, importantly, epiblast-specific translation of its mRNA. These functions were established when 213 bp of the 5′ UTR and the 3′ UTR were fused to the *otd* coding sequence. We have recently reported that mice carrying a 300 bp insertion in the *Otx2*-3′ UTR exhibited epiblast-restricted impairment in the translation of the mutated *Otx2* mRNA (Pilo Boyl et al., 2001). Here we have also shown that *hOtx1*^{2} mutants, which lack the same *Otx2* sequences that were absent in *otd*^{2} mutants, display identical molecular impairments. Together these data provided in vivo evidence of both gain and loss of protein synthesis in epiblast and neuroectoderm, depending on the presence of 5′ and 3′ UTRs of *Otx2*. While we have reported that the 3′ UTR may be relevant in the translation of the *Otx2* mRNA (Pilo Boyl et al., 2001), we believe that also the 5′ UTR plays an important role in this control. This is supported by preliminary data indicating that mice lacking only 150 bp within the 213 bp long region deleted in *otd* mutants, develop a sharp headless phenotype (D. A. and A. S., unpublished results).

In sum, these data support the notion that *otd/Otx* functions have been established in a common ancestor of fly and mouse and retained throughout evolution, while regulatory control of their expression has been modified and re-adapted by evolutionary events that have led to the specification of the increasingly complex vertebrate brain (Sharman and Brand, 1998; Simeone, 1998; Acampora and Simeone, 1999; Reichert and Simeone, 1999).

A likely consequence of modification of regulatory control of gene expression may result in a greater number of molecular interactions. This may contribute to modifying relevant morphogenetic processes that, in turn, can confer a change in shape and size of the body plan as well as in the generation of cell types with new developmental potentials (Holland, 1999; Acampora and Simeone, 1999). On this basis, *Otx* gene duplication and subsequent or contemporary modification of regulatory control might have contributed to the evolution of the mammalian brain, for example by controlling the position of the midbrain-hindbrain boundary (MHB).

Previous work has indicated that *Otx* genes control the positioning of MHB (Simeone, 2000; Wurst and Bally-Cuif, 2001). Importantly, this control is strictly dependent on the level of OTX proteins in the neuroectoderm. Data presented in this study and those previously reported, clearly indicate that reduction in OTX levels is invariably reflected in anterior displacement of the MHB and progressive loss of forebrain and midbrain identities. Our data demonstrate that OTD protein may restore a quite normal positioning of the MHB, thus indicating that a crucial process in murine brain development can be performed by the invertebrate function.

Nevertheless, this process may occur only if the *Otx2* regulatory control is provided. On this basis, we hypothesise that, once established, this control has been recruited and maintained throughout vertebrate head evolution.

We wish to thank Andrew Lumsden for critical reading of the manuscript and helpful discussions. We also thank A. Secondulfo and S. Piga for manuscript preparation, Amanda McGuigan and the staff for the excellent animal care. This work was supported by the MRC (Grant Number: G9900955), the Wellcome Trust (Grant Number: 062642/Z/00), the Italian Association for Cancer Research (AIRC), the EU BIOTECH programme (Number: BIO4-CT98-0309), the CNR Target Project on Biotechnology, the MURST-CNR Programme Legge 488/92 (cluster 02) and the Fondation Bettencourt Schueller.

REFERENCES

Acampora, D. and Simeone, A. (1999). Understanding the roles of *Otx1* and *Otx2* in controlling brain morphogenesis. *Trends Neurosci.* **22**, 116-122.

Acampora, D., Mazan, S., Lallemand, Y., Avantaggiato, V., Maury, M., Simeone, A. and Brûlet, P. (1995). Forebrain and midbrain regions are deleted in *Otx2*$^{-/-}$ mutants due to a defective anterior neuroectoderm specifiction during gastrulation. *Development* **121**, 3279-3290.

Acampora, D., Mazan, S., Avantaggiato, V., Barone, P., Tuorto, F., Lallemand, Y., Brûlet, P. and Simeone, A. (1996). Epilepsy and brain abnormalities in mice lacking *Otx1* gene. *Nature Genet.* **14**, 218-222.

Acampora, D., Avantaggiato, V., Tuorto, F. and Simeone, A. (1997). Genetic control of brain morphogenesis through *Otx* gene dosage requirement. *Development* **124**, 3639-3650.

Acampora, D., Avantaggiato, V., Tuorto, F., Barone, P., Reichert, H., Finkelstein, R. and Simeone, A. (1998a). Murine *Otx1* and *Drosophila otd* genes share conserved genetic functions required in invertebrate and vertebrate brain development. *Development* **125**, 1691-1702.

Acampora, D., Avantaggiato, V., Tuorto, F., Briata, P., Corte, G. and

Simeone, A. (1998b). Visceral endoderm-restricted translation of *Otx1* mediates recovering of *Otx2* requirements for specification of anterior neural plate and proper gastrulation. *Development* **125**, 5091-5104.

Acampora, D., Avantaggiato, V., Tuorto, F., Barone, P., Perera, M., Choo, D., Wu, D., Corte, G. and Simeone, A. (1999). Differential transcriptional control as the major molecular event in generating *Otx1*$^{-/-}$ and *Otx2*$^{-/-}$ divergent phenotypes. *Development* **126**, 1417-1426.

Acampora, D., Gulisano, M., Broccoli, V. and Simeone, A. (2001). *Otx* genes in brain morphogenesis. *Prog. Neurobiol.* **64**, 69-95

Ang, S.-L., Jin, O., Rhinn, M., Daigle, N., Stevenson, L. and Rossant, J. (1996). Targeted mouse *Otx2* mutation leads to severe defects in gastrulation and formation of axial mesoderm and to deletion of rostral brain. *Development* **122**, 243-252.

Araki, I. and Nakamura, H. (1999). *Engrailed* defines the position of dorsal di-mesencephalon boundary by repressing diencephalic fate. *Development* **126**, 5127-5135.

Arendt, D. and Nübler-Jung, K. (1996). Common ground plans in early brain development in mice and flies. *BioEssays* **18**, 255-259.

Arendt, D. and Nübler-Jung, K. (1999). Comparison of early nerve cord development in insects and vertebrates. *Development* **126**, 2309-2325.

Beddington, R. S. and Robertson, E. J. (1999). Axis development and early asymmetry in mammals. *Cell* **96**, 195-209.

Briata, P., Di Blas, E., Gulisano, M., Mallamaci, A., Iannone, R., Boncinelli, E. and Corte, G. (1996). EMX1 homeoprotein is expressed in cell nuclei of the developing cerebral cortex and in the axons of the olfactory sensory neurons. *Mech. Dev.* **57**, 169.

Callaerts, P., Halder, G. and Gehring, W. J. (1997). *Pax-6* in development and evolution. *Annu. Rev. Neurosci.* **20**, 483-532.

De Robertis, E. M. and Sasai, Y. (1996). A common plan for dorsoventral patterning in the Bilateria. *Nature* **380**, 37-40.

Finkelstein, R. and Boncinelli, E. (1994). From fly head to mammalian forebrain: the story of *otd* and *Otx*. *Trends Genet.* **10**, 310-315.

Garstang, W. (1928). The morphology of the Tunicata, and its bearing on the phylogeny of the Chordata. *Q. J. Microsc. Sci.* **72**, 51-187.

Hanks, M. C., Loomis, C. A., Harris, E., Tong, C.-X., Cartwright, L., Auerbach, A. and Joyner, A. (1998). *Drosophila engrailed* can substitute for mouse *Engrailed1* function in mid-hindbrain, but not limb development. *Development* **125**, 4521-4530.

Hogan, B., Beddington, R., Costantini, F. and Lacy, E. (1994). In *Manipulating the Mouse Embryo. A Laboratory Manual.* 2nd edn. Cold Spring Harbor, NY: Cold Spring Harbor Laboratory Press.

Holland, P. W. H. (1999). The future of evolutionary developmental biology. *Nature* **402 Suppl**. C41-C44.

Joyner, A. L. (1996). *Engrailed*, *Wnt* and *Pax* genes regulate midbrain-hindbrain development. *Trends Genet.* **12**, 15-20.

Krumlauf, R. (1994). *Hox* genes in vertebrate development. *Cell* **78**, 191-201.

Lacalli, T. (1994). Apical organs, epithelial domains, and the origin of the chordate central nervous system. *Amer. Zool.* **34**, 533-541.

Lemaire, P. and Kodjabachian, L. (1996). The vertebrate organizer: structure and molecules. *Trends Genet.* **12**, 525-531.

Leuzinger, S., Hirth, F., Gerlich, D., Acampora, D., Simeone, A., Gehring, W., Finkelstein, R., Furukubo-Tokunaga, K. and Reichert, H. (1998). Equivalence of the fly *orthodenticle* gene and the human *OTX* genes in embryonic brain development of *Drosophila*. *Development* **125**, 1703-1710.

Lewis, E. B. (1978). A gene complex controlling segmentation in *Drosophila*. *Nature* **276**, 565-570.

Li, Y., Allende, M. L., Finkelstein, R. and Weinberg, E. S. (1994). Expression of two zebrafish *orthodenticle*-related genes in the embryonic forebrain. *Mech. Dev.* **48**, 229-244.

Liu, A., Losos, K. and Joyner, A. L. (1999). FGF8 can activate gbx2 and ransform regions of the rostral mouse brain into a hindbrain fate. *Development* **126**, 4827-4838.

Loreni, F. and Amaldi, F. (1992). Translational regulation of ribosomal protein synthesis in *Xenopus* cultured cells: mRNA relocation between polysomes and RNA during nutritional shifts. *Eur. J. Biochem.* **205**, 1027-1032.

Lumsden, A. (1990). The cellular basis of segmentation in the developing hindbrain *Trends Neurosci.* **13,** 329-335.

Lumsden, A. and Krumlauf, R. (1996). Patterning the vertebrate neuraxis. *Science* **274**, 1109-1115.

Matsuo, I., Kuratani, S., Kimura, C., Takeda, N. and Aizawa, S. (1995). Mouse *Otx2* functions in the formation and patterning of rostral head. *Genes Dev.* **9**, 2646-2658.

Morsli, H., Tuorto, F., Choo, D., Posiglione, M. P., Simeone, A. and Wu, D. K. (1999). *Otx1* and *Otx2* activities are required for the normal development of the mouse iner ear. *Development* **126**, 2335-2343.

Nagao, T., Leuzinger, S., Acampora, D., Simeone, A., Finkelstein, R., Reichert, H. and Furukubo-Tokunaga, K. (1998). Developmental rescue of *Drosophila* cephalic defects by the human *Otx* genes. *Proc. Natl. Acad. Sci. USA* **95**, 3737-3742.

Peterson, K. J. (1995). Dorsoventral axis inversion. *Nature* **373**, 111-112.

Pilo Boyl, P., **Signore, M., Acampora, D., Martinez-Barbera, J. P., Ilengo, C., Annino, A., Corte, G. and Simeone, A.** (2001). Fore-midbrain development requires epiblast-restricted *Otx2* translational control mediated by its 3′ UTR. *Development* **128**, 2989-3000.

Reichert, H. and Simeone, A. (1999). Conserved usage of gap and homeotic genes in patterning the CNS. *Curr. Opin. Neurobiol.* **9**, 589-595.

Rhinn, M., Dierich, A., Shawlot, W., Behringer, R. R., Le Meur, M. and Ang, S.-L. (1998). Sequential roles for *Otx2* in visceral endoderm and neuroectoderm for forebrain and midbrain induction and specification. *Development* **125**, 845-856.

Rubenstein, J. L. R., Shimamura, K., Martinez, S. and Puelles, L. (1998). Regionalization of the prosencephalic neural plate. *Annu. Rev. Neurosci.* **21**, 445-477.

Sharman, A. C. and Brand, M. (1998). Evolution and homology of the nervous system: cross-phylum rescues of *otd/Otx* genes. *Trends Genet.* **14**, 211-214.

Simeone, A. (1998). *Otx1* and *Otx2* in the development and evolution of the mammalian brain. *EMBO J.* **17**, 6970-6978.

Simeone, A. (1999). Detection of mRNA in tissue sections with radiolabelled riboprobes. In *In Situ Hybridization. A Practical Approach.* 2nd edition (ed. D. G. Wilkinson), pp. 69-86, Oxford: IRL, Oxford University Press.

Simeone, A. (2000). Positioning the isthmic organizer where *Otx2* and *Gbx2* meet. *Trends Genet.* **16**, 237-240.

Simeone, A., Acampora, D., Gulisano, M., Stornaiuolo, A. and Boncinelli, E. (1992). Nested expression domains of four homeobox genes in developing rostral brain. *Nature* **358**, 687-690.

Simeone, A., Acampora, D., Mallamaci, A., Stornaiuolo, A., D'apice, M. R., Nigro, V. and Boncinelli, E. (1993). A vertebrate gene related to *orthodenticle* contains a homeodomain of the *bicoid* class and demarcates anterior neuroectoderm in the gastrulating mouse embryo. *EMBO J.* **12**, 2735-2747.

Suda, Y., Matsuo, I. and Aizawa, S. (1997). Cooperation between Otx1 and Otx2 genes in developmental patterning of rostral brain. *Mech. Dev.* **69**, 125-141.

Wurst, W. and Bally-Cuif, L. (2001). Neural plate patterning: upstream and downstream of the isthmic organizer. *Nature Rev. Neurosci.* **2,** 99-108